BIOMOLECULES & THERAPEUTICS

Original Article
Biomol Ther 31(1), 116-126 (2023)

Minoxidil Regulates Aging-Like Phenotypes in Rat Cortical Astrocytes *In Vitro*

Minji Bang[1,2], Seung Jin Yang[3], TaeJin Ahn[3], Seol-Heui Han[4], Chan Young Shin[2] and Kyoung Ja Kwon[2,4,*]

[1]*Biological Science, College of Science & Technology, Dankook University, Cheonan 31116,*
[2]*Department of Neuroscience and Pharmacology, School of Medicine, Konkuk University, Seoul 05029,*
[3]*Department of Life Science, Handong Global University, Pohang 37554,*
[4]*Department of Neurology, Konkuk Hospital Medical Center, Seoul 05030, Republic of Korea*

Abstract

Mainly due to the slanted focus on the mechanism and regulation of neuronal aging, research on astrocyte aging and its modulation during brain aging is scarce. In this study, we established aged astrocyte culture model by long-term culturing. Cellular senescence was confirmed through SA-β-gal staining as well as through the examination of morphological, molecular, and functional markers. RNA sequencing and functional analysis of astrocytes were performed to further investigate the detailed characteristics of the aged astrocyte model. Along with aged phenotypes, decreased astrocytic proliferation, migration, mitochondrial energetic function and support for neuronal survival and differentiation has been observed in aged astrocytes. In addition, increased expression of cytokines and chemokine-related factors including plasminogen activator inhibitor -1 (PAI-1) was observed in aged astrocytes. Using the RNA sequencing results, we searched potential drugs that can normalize the dysregulated gene expression pattern observed in long-term cultured aged astrocytes. Among several candidates, minoxidil, a pyrimidine-derived anti-hypertensive and anti-pattern hair loss drug, normalized the increased number of SA-β-gal positive cells and nuclear size in aged astrocytes. In addition, minoxidil restored up-regulated activity of PAI-1 and increased mitochondrial superoxide production in aged astrocytes. We concluded that long term culture of astrocytes can be used as a reliable model for the study of astrocyte senescence and minoxidil can be a plausible candidate for the regulation of brain aging.

Key Words: Astrocytes, Brain aging, Mitochondria, Transcriptomic profiling, Minoxidil

INTRODUCTION

Aging is one of the biggest problems in human society at the moments with the rapidly growing elderly population and the research on aging as well as geriatric diseases has uppermost importance. Therefore, delineating the mechanisms of aging-related changes in cellular functions would be the first step to understand aging and to devise the methods to regulate aging and aging-related diseases. It is obvious that each cell types in the brain including neurons and astrocytes would undergo cell type-specific aging process. Therefore, it is both necessary and important to study the aging process and the mechanism underlying it at the level of each cell types. However, most of the aging studies involving central nervous system (CNS) have been focused on neurons or microglia. This may pose a problem in the interpretation of aging process in the brain considering the magnitude of the cell population and proliferation potency of the other important cell types, i.e. astrocytes. For example, a decrease in brain volume is observed as one of the characteristics of brain aging, but Freeman *et al*. (2008) reported that number of neurons was not changed in elderly subjects nor Alzheimer's disease patients. The brain atrophy with aging may be mediated by the dysregulation of glial cells, especially astrocytes. Astrocytes are the largest cell population in the brain with proliferation potential and are well known to exert various functions ranging from structural maintenance of the brain to functional regulation of neurotransmission (Chung *et al*., 2015; Burda *et al*., 2016; Siracusa *et al*., 2019). In addition, astrocytes have a direct effect on neuronal survival and development by secreting neurotrophic factors, assisting cell growth and survival, and contributing to neuronal signal transmission by regulating the concentration of neu-

Open Access **https://doi.org/10.4062/biomolther.2022.144**

Received Nov 10, 2022 **Revised** Nov 24, 2022 **Accepted** Nov 25, 2022
Published Online Dec 20, 2022

***Corresponding Author**
E-mail: neuro11@kku.ac.kr
Tel: +82-2-454-5630, Fax: +82-2-548-5630

rotransmitters at synapses (Fiacco *et al*., 2009). In particular, astrocytes regulate the immune activity in the brain along with microglia, and it is relatively well known that astrocytes and microglia exhibit a mild inflammatory phenotypes with aging (Abbott *et al*., 2006).

With the multitude of the function served by the astrocytes, functional dysregulation of astrocytes with aging may also affect various other brain cells resulting in the dysregulation of the maintenance of the optimal brain environment (Dossi *et al*., 2018).

In this study, we developed an *in vitro* astrocyte aging model by culturing the cells for a long time more than 12 weeks for in-depth study on astrocyte aging and screening of drug candidates with potential to control astrocyte and brain aging processes, which may ultimately be used against neurodegenerative disorders such as Alzheimer's disease and Parkinson's disease. We analyzed functional changes of senescent astrocytes in detail and searched for putative senescence regulators through transcriptomic profiling and connectivity map (CMap) analysis (Lamb *et al*., 2006). Here, we report that long-term culture of astrocytes shows cellular senescent phenotypes along with functional deficits, which even affect deficits in neural support by astrocytes. The potential use of minoxidil as a modulator of astrocyte senescence will be demonstrated.

MATERIALS AND METHODS

Materials

The materials used in this study are as follows: Dulbecco's modified Eagle medium (DMEM)/F12, Penicillin-Streptomycin (P/S), 0.25% trypsin-EDTA, and 10% Fetal Bovine Serum (FBS) were from Gibco BRL (Grand Island, NY, USA); Tween® 20 and ECLTM Western blotting detection reagent were from Amersham Life Science (Arlington Heights, IL, USA); anti-β Actin was obtained from Sigma (St. Louis, MO, USA); anti-iNOS and senescence detection kit were the product of Abcam (Cambridge, UK); minoxidil was obtained from Sigma; Agilent Seahorse XF Cell Mito Test Kit was from Agilent Technologies (CA, USA); Alexa Fluor® 594 conjugated Escherichia coli (K-12 strain) BioParticles® and Tetramethylrhodamine Methyl Ester (TMRM) were purchased from Thermo Fisher Scientific (MA, USA); MitoSOX™ was from Invitrogen (MA, USA).

Astrocyte culture

Animal maintenance and experimental processes were performed following the rules and conditions approved by the Institutional Animal Care and Use Committee (IACUC) of Konkuk University (KU19017). Sprague-Dawley (SD) rats were purchased from Samtako, Inc. (Osan, Korea). Astrocytes were cultured from brain cortex of postnatal day 2 (P2) SD rats as described previously (Bang *et al*., 2019b). Concisely, brain cortices were dissected and mechanically triturated. The triturated cells were plated on the poly-D-lysine-coated plate (20 μg/mL) and incubated in DMEM/F12 with 100 U/mL of penicillin, 100 mg/mL of streptomycin, and 10% heat-inactivated FBS in a 95% CO_2 incubator at 37°C. The culture medium was changed every 3 or 4 days. After 2 or 12 weeks, the incubated astrocytes were sub-cultured in the well plates. The purity of sub-cultured astrocyte was more than 95% as determined by counting the glial fibrillary acidic protein (GFAP) positive cells.

Neuron culture

Pregnant Sprague-Dawley (SD) rats were purchased from ORIENT (Seongnam, Korea). The primary neurons were dissected from the cortex of embryonic day 18 (E18) SD rats. The isolated cortical neurons were mechanically triturated and seeded on the poly-D-lysine-coated plate (50 μg/mL). The seeded cells were maintained in NBM with B27 supplement and L-glutamine in a 95% CO_2 incubator at 37°C. The media were half-changed every 3 days.

Senescence-associated-β-galactosidase (SA-β-gal) staining

SA-β-gal positive cells were detected using Senescence Detection Kit (Abcam) *in vitro*. The experiment was proceeded following the manufacturer's instructions (Dimri *et al*., 1995). Density of astrocytes was 2.5×10^5 cells in 12 well-plate.

Nuclear staining

Cells were incubated on a poly-D-lysine-coated coverslip and were fixed by 4% paraformaldehyde (PFA) for 10 min at 37°C. After then, the cells were permeabilized by 0.1% Triton X-100 for 20 min at room temperature. The fixed cells were stained by DAPI (4′,6-diamidino-2-phenylindole) for 10 min at room temperature. The samples were mounted with GEL/MOUNT (Biomeda Corp., CA, USA) and visualized by a digital microscope (CELENA, Logos Biosystems, Anyang, Korea).

Reverse transcription-polymerase chain reaction (RT-PCR)

The RNA isolation was conducted with TRIzol reagent (Invitrogen). The concentration of extracted RNA was measured using a spectrophotometer (Nanodrop Technologies, Wilmington, DE, USA). The RNA was used for the synthesis of cDNA with RT reaction mixture containing RevertAid Reverse transcriptase reaction buffer (Thermo Fisher Scientific) and dNTP (Promega, WI, USA). cDNA was used as template for PCR amplification with following protocol: [94°C, 30 s; 60°C, 1 min; 72°C, 30 s]×30 cycles, then 72°C for 10 min; or [94°C, 30 s; 60°C, 1 min; 72°C, 30 s]×23 cycles, then 72°C for 10 min. The sequences of primers used in this study are as follows: *IL-1β* (sense: 5'-AAA ATG CCT CGT GCT GTC TG-3'/ antisense: 5'-CTA TGT CCC GAC CAT TGC TG-3'), *IL-6* (sense: 5'-TTG TGC AAT GGC AAT TCT GA-3'/ antisense: 5'-TGG AAG TTG GGG TAG GAA GG-3'), *iNOS* (sense: 5'-CTG GCT GCC TTG TTC AGC TA-3'/ antisense: 5'-AGT GTA GCG TTT CGG GAT CT-3'), *p16* (sense: 5'-ATC TCC GAG AGG AAG GCG AAC TCG-3'/ antisense: 5'-TCT GTC CCT CCC TCC CTC TGC TAA C-3') and *GAPDH* (sense: 5'-GTG AAG GTC GGT GTG AAC GGA TTT-3'/ antisense: 5'-CAC AGT CTT CTG AGT GGC AGT GAT-3'). The PCR products were normalized by GAPDH or 18s RNA mRNA.

Western blot analysis

Western blot experiment was conducted following a previously described procedure (Bang *et al*., 2019b). Briefly, cells were harvested with radioimmunoprecipitation assay (RIPA) buffer containing 2 mM EDTA, 0.1% (w/v) SDS, 50 mM Tris-HCl, 150 mM sodium chloride, 1% Triton X-100, and 1% (w/v) sodium deoxycholate. Concentration of the proteins was measured by BCA assay kit (Thermo Fisher Scientific). The proteins samples in SDS-PAGE buffer were boiled for 5 min at 100°C. The SDS-PAGE was performed for 120 min at 100 V. The proteins were electrically transferred to nitrocellulose

membranes for 90 min and were blocked with 1 μg/mL polyvinyl alcohol for 5 min at room temperature. After then, samples were washed 3 times for 5 min with Tris-buffered saline and 0.1% Tween 20 (TBS-T). The proteins attached blots were incubated with primary antibodies for 16 h at 4°C. The blots were washed and maintained with horseradish peroxidase-conjugated secondary antibody (Life Technologies, Carlsbad, CA, USA) at room temperature for 60 min. The expression of proteins was visualized by a chemiluminescence detection system (Amersham, Buckinghamshire, UK) and quantified using Image-J software (NIH, USA). The intensity of the bands was normalized using β-Actin as control.

Inverse casein zymography

The plasminogen activator inhibitor-1 (PAI-1) activity was measured through inverse casein zymography following previously described methods (Ko *et al*., 2015). Briefly, cultured media supernatant of cells was mixed with SDS-PAGE sample buffer lacking β-mercaptoethanol. The samples were conducted SDS-PAGE using gels containing casein and then, gels were rinsed twice in 2.5% Triton X-100 for 30 min. The gels were gently shaken for 5 h at 25°C in reaction buffer (20 mM Tris–HCl, pH 7.6). containing urokinase-type plasminogen activator (uPA; 0.5 IU/mL; American Diagnostica, NY, USA). After then, the inverse-zymography gels were stained with 0.1% Coomassie brilliant blue R-250 (Elpisbio, Daejeon, Korea) and de-stained with de-staining buffer containing 20% methanol and 10% acetic acid. The gels were visualized using the LAS4000 image detection system (Fuji, Tokyo, Japan).

Wound closure assay

Confluent cells were scratched 700 nm-wide using a certified Essen Bioscience automated 96-wound-maker™ (Essen Bioscience, Hertfordshire, UK). Wound width and density were measured using the IncuCyte ZOOM system (Essen Bioscience, MI, USA) and were analyzed using the IncuCyte ZOOM microscope software 2015A (Essen Bioscience).

Phagocytosis

Alexa Fluor™ 594 conjugated *Escherichia coli* (K-12 strain) BioParticles™ were incubated with cells and the red fluorescence inside the cells was measured by the IncuCyte ZOOM system (Essen Bioscience) every 30 min for 12 h. The images were analyzed by the IncuCyte ZOOM microscope software 2015A (Essen Bioscience).

Determination of mitochondrial membrane potential

The cells were incubated with 100 nM TMRM staining solution in light protection conditions for 30 min at 37°C. After then, the cells were rinsed with phosphate-buffered saline (PBS) and imaged by the IncuCyte ZOOM system (Essen Bioscience). The images were analyzed by the IncuCyte ZOOM microscope software 2015A (Essen Bioscience).

Mitochondrial oxygen consumption rate (OCR)

The measurement of mitochondrial OCR was proceeded following the Agilent Seahorse XF Cell Mito Test Kit user guide. Briefly, the sensor cartridges were incubated overnight with a calibrant buffer in a non-CO_2 incubator at 37°C. Mitochondrial modulators such as 1.0 μM oligomycin, 1.0 μM FCCP, or 0.5 μM rotenone/0.5 μM antimycin A were put in each port of cartridge as instructed. The cells were incubated with Seahorse XF Base Medium containing 1 mM pyruvate, 2 mM glutamine, and 10 mM glucose for about 1 h. Mitochondrial OCR was measured by Agilent Seahorse XFe96 Analyzer. The results were analyzed by Wave Desktop 2.6 software (Santa Clara, CA, USA).

Measurement of neurite outgrowth

Astrocyte cultured media (ACM) were harvested from astrocyte cultured for 24 h in serum free condition. The rat cortical neurons were incubated for 2 days and added with ACM obtrained from young and aged culture. The length of the neurite was measured using the IncuCyte® Live-Cell Analysis system (Essen BioScience, Inc., Ann Arbor, MI, USA).

RNA-sequencing

Astrocytes were incubated for 2 or 12 weeks and sub-cultured. The sub-cultured astrocytes were treated with vehicle (DPBS; Dulbecco's Phosphate-Buffered Saline) or 10 ng/mL lipopolysaccharide (LPS) and harvested with trizol. The samples were used for RNA-sequencing by a commercial sequencing company (Macrogen, Seoul, Korea).

Measurement of mitochondrial superoxide

The cells were incubated with 5 μM MitoSOX™ (Invitrogen) for 10 min at 37°C, protected from light. The samples were washed gently 3 times. The level of mitochondrial superoxide was measured using the IncuCyte® Live-Cell Analysis system.

Statistical analysis

All the experimental data were presented as the mean ± SEM and the statistical analyses were performed using GraphPad Prism version 5 software (GraphPad Software Inc., CA, USA). The group comparisons were conducted using two-way ANOVA followed by Bonferroni's post-test. Two-sample comparison was analyzed with unpaired t-test. A *p*-value of <0.05 was considered significant.

RESULTS

Long-term cultured astrocytes displayed aged cell-like phenotypes

Astrocytes were incubated for 2 (short-term cultured astrocytes) or 12 (long-term cultured astrocytes) weeks. Cells were stained with SA-β-gal to confirm whether long-term cultured astrocytes show cellular senescence phenotype. Usually, astrocytes are cultured for 2 weeks and are used for experiments. To establish senescent cells, astrocytes were cultured for 4, 8, 10, 12, 16 and 20 weeks (data not shown). While astrocyte cultures exceeding 16-week period separated from the culture plate, cells cultured for less than 10 weeks did not show a senescent phenotype. As a result, we found that 12-week cultured astrocytes could be maintained for the longest time without being separated from the culture plate. Long-term cultured astrocytes displayed SA-β-gal positive cells 11 times more than short-term cultured astrocytes (Fig. 1A). Senescent cells exhibit nucleus enlargement phenotype (Yoon *et al*., 2016), therefore, the nuclear size of astrocytes was measured using DAPI staining. After photographing DAPI-stained nuclei, the number of pixels was counted using the Image-J software program. The nuclear size of long-term cultured astrocytes was 17% larger than that of short-term cultured astrocytes

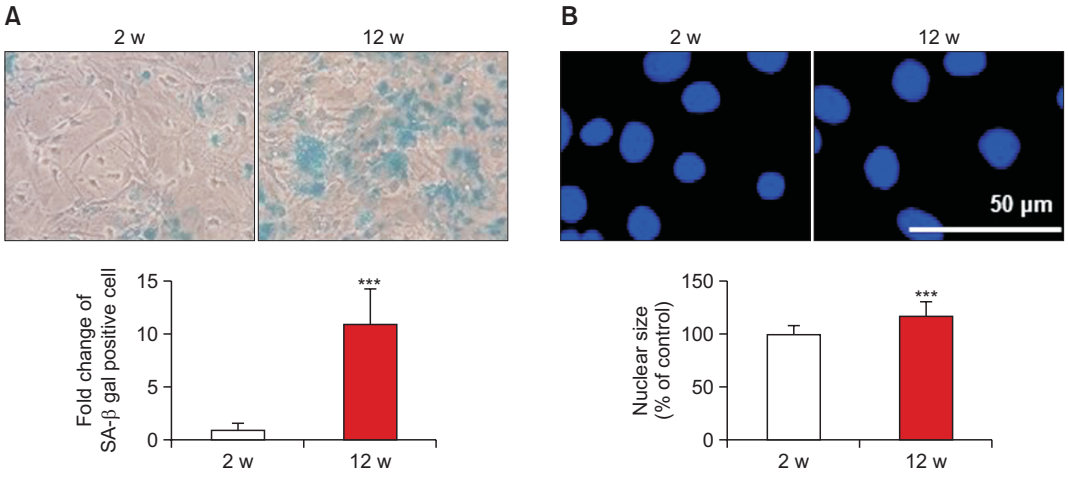

Fig. 1. Morphological changes of long-term cultured astrocytes. (A) Cultured astrocytes were with stained senescence-associated beta-galactosidase (SA-β-gal). The bar graph shows fold changes of SA-β-gal positive cell number. (B) Cultured astrocytes were indicated by DAPI to determine size of nuclei. The bar graph representative nuclei size of cells. ***p<0.001 vs. short-term cultured astrocytes. The data analysis was performed using unpaired t-test and Error bars indicate SD.

(Fig. 1B). Taken together, these results suggest that long-term culture of astrocytes exhibit morphological phenotypes of senescent cells.

To determine whether long-term cultured astrocytes show the molecular phenotypes of senescent cells as well, we first performed RT-PCR to detect mRNA expression, which has been implicated in cellular senescence. Those senescence-related factors include immune- and cell cycle-related factors as well as protease-related factors. In this study, the expression level of *IL-1b* and *IL-6* was significantly increased in long-term cultured astrocytes in basal, non-stimulated condition (Fig. 2A). In addition, the mRNA expression of *p16*, a tumor suppressor and a well-known biomarker of cellular senescence, was increased 1.5-folds in long-term cultured astrocytes (Fig. 2B). To mimic the immune-challenged situation, we stimulated long-term cultured astrocytes with 0 (DPBS), 1, or 10 ng/mL LPS (Fig. 2C, 2D). Although *iNOS* mRNA and protein expression levels were not detected under basal conditions, immune activation increased the expression of iNOS which is more prominent in long-term cultured astrocytes compared with short-term cultured astrocytes (Fig. 2C). Increased *PAI-1* mRNA expression level was also observed in long term cultured astrocytes (Fig. 2D). Inverse-zymography and Western blot also showed increased activity and protein expression levels of PAI-1, respectively, in long-term cultured astrocytes (Fig. 2E, 2F).

To identify functional significance of the astrocyte senescent phenotypes, astrocyte migration, phagocytosis, and mitochondrial function were examined. Migration of cells was investigated through wound-scratch assay. After making scratch wound with a width of about 700-800 μm on the confluent astrocyte cultures, the width and density of wound were automatically determined using computer-aided analytical tools (Incucyte, Essen Bioscience). Wound closure of long-term cultured astrocytes was significantly slower than cells cultured for short-term (Fig. 3A). The rate of decrease in wound width was slower in long-term cultured cells and the relative cell density in wound, which represents the cell density in the wound area compared to the cell density outside the wound area that changes over time, was higher in the short-term cultured cells compared to the long-term cultured cells. Next, phagocytosis function of astrocytes was investigated using *E. coli* bio-particles uptake assay. The intensity of *E. coli* bio-particles inside the cells was decreased in long-term cultured astrocytes, suggesting the reduced phagocytotic activity of the aged cells (Fig. 3B). To identify mitochondrial function of long-term cultured astrocytes, mitochondrial membrane potential was determined using TMRM. Doxorubicin, a well-known mitochondrial toxin, was used as a positive control. Long-term cultured astrocytes showed significantly reduced TMRM intensity compared to short-term cultured astrocytes (Fig. 3C). In addition, spare respiratory capacity was increased in long-term cultured astrocytes (Fig. 3D) although no differences in basal respiration, proton leak and ATP production were observed between short- and long-term cultured astrocytes.

Conditioned media from long-term cultured astrocytes show altered capacity to support neurons

Astrocytes and neurons interact closely, and consequently, we reasoned that dysfunction of astrocytes in long-term culture could adversely affect neuronal function such as neurite outgrowth and mitochondrial OCR (Lee *et al*., 2020; Zhang *et al*., 2022). Thus, we tried to examine the effects of long-term cultured astrocytes on neuron through the application of astrocyte culture-conditioned media (ACM) to neuron. After applying ACM to neuron, neurite outgrowth was monitored and analyzed every 3 h. Control ACM treated neurons displayed longer length of neurite than non-treated group. However, long-term cultured ACM treated neurons measured shorter neurite length than short-term cultured ACM treated neurons (Fig. 4A). In mitochondrial OCR experiment of long-term cultured ACM treated neurons, spare respiratory capacity of neuron was increased (Fig. 4B) suggesting that the long-term cultured astrocytes adversely affect their capability to modulate neuronal function.

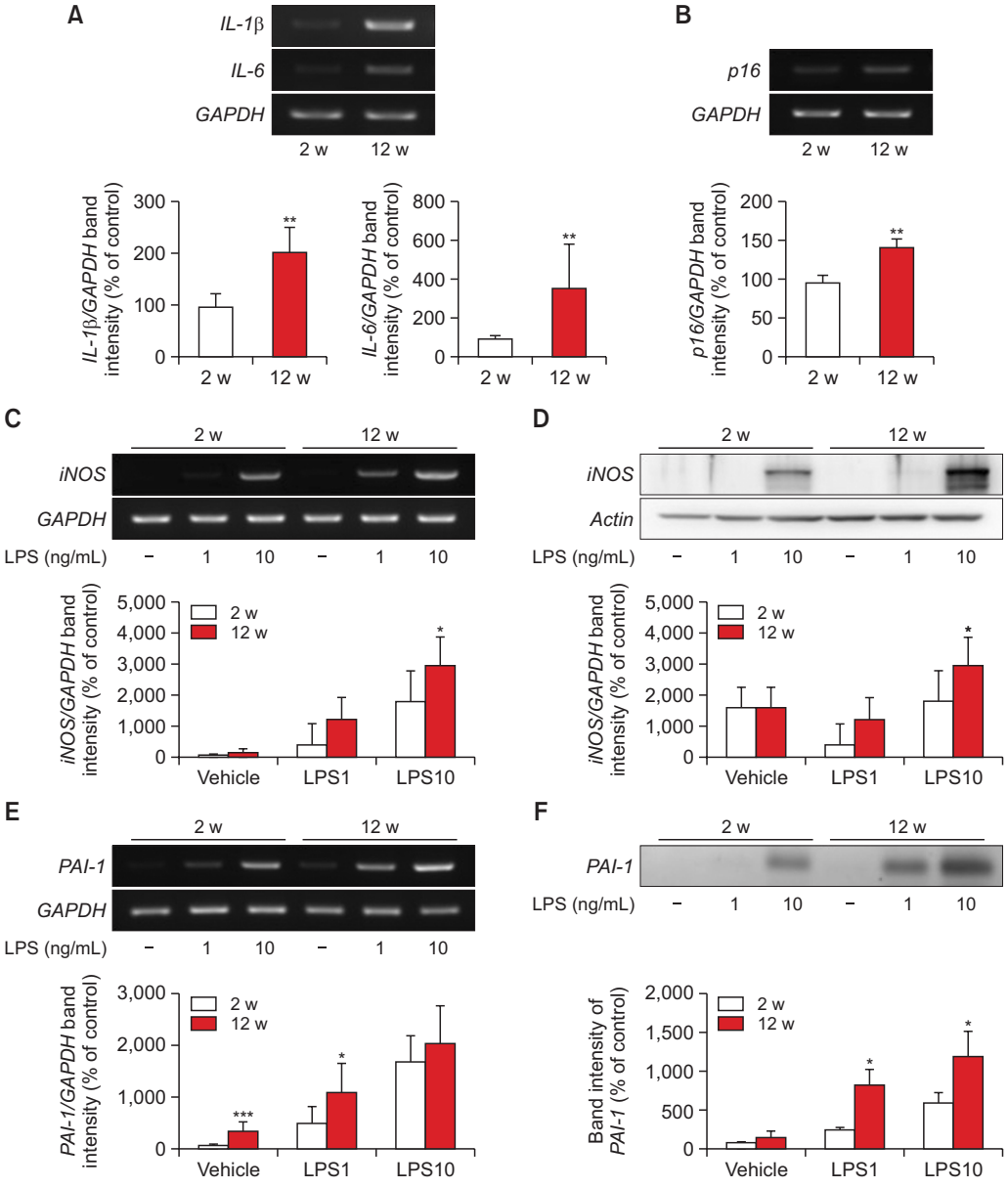

Fig. 2. Molecular changes of long-term cultured astrocytes. Cultured astrocytes were treated with 0 (vehicle), 1, 10 ng/mL lipopolysaccharides (LPS) for 24 h. The graph represents mRNA expression of (A) immune-related genes and a (B) cell-cycle-related gene. The level of mRNA expression was measured by reverse transcription PCR (RT-PCR) and was normalized by the expression level of GAPDH. (C) RT-PCR and (D) western blot was performed for measuring expression levels of iNOS gene and protein. The results of protein expression were normalized based on actin expression. (E) The PAI-1 mRNA and (F) protein activity were confirmed through RT-PCR and inverse-zymography. *p<0.05, **p<0.01, and ***p<0.001 vs. short-term cultured astrocytes (each treated groups). The group comparisons were conducted using two-way ANOVA followed by Bonferroni's post-test. Two-sample analyses were analyzed with unpaired t-test. And Error bars indicate SD.

Gene expression signature of long-term cultured astrocytes

RNA-seq was performed to examine the gene expression profile of long-term cultured astrocytes and comparative transcriptome analysis was performed according to the workflow in Fig. 5A. The gene ontology of the selected target gene was identified through GENE MENIA and GOrilla. Genes which showed a significant change (38 up-regulated genes, and 64 down-regulated genes ($|\log_2 FC|>1.5$, p-value <0.05) in long-term culture, were further analyzed for the prediction of function of gene sets through GENE MENIA analysis and the related cellular components were analyzed using GOrilla. Genes that were significantly increased by long-term culture showed a substantial correlation with the extracellular region, and the significantly decreased gene set exhibited a high correlation with the membrane (Supplementary Fig. 1A, 1B).

In addition, CMap was performed to find perturbagens showing opposite phenotype to the changes in gene expres-

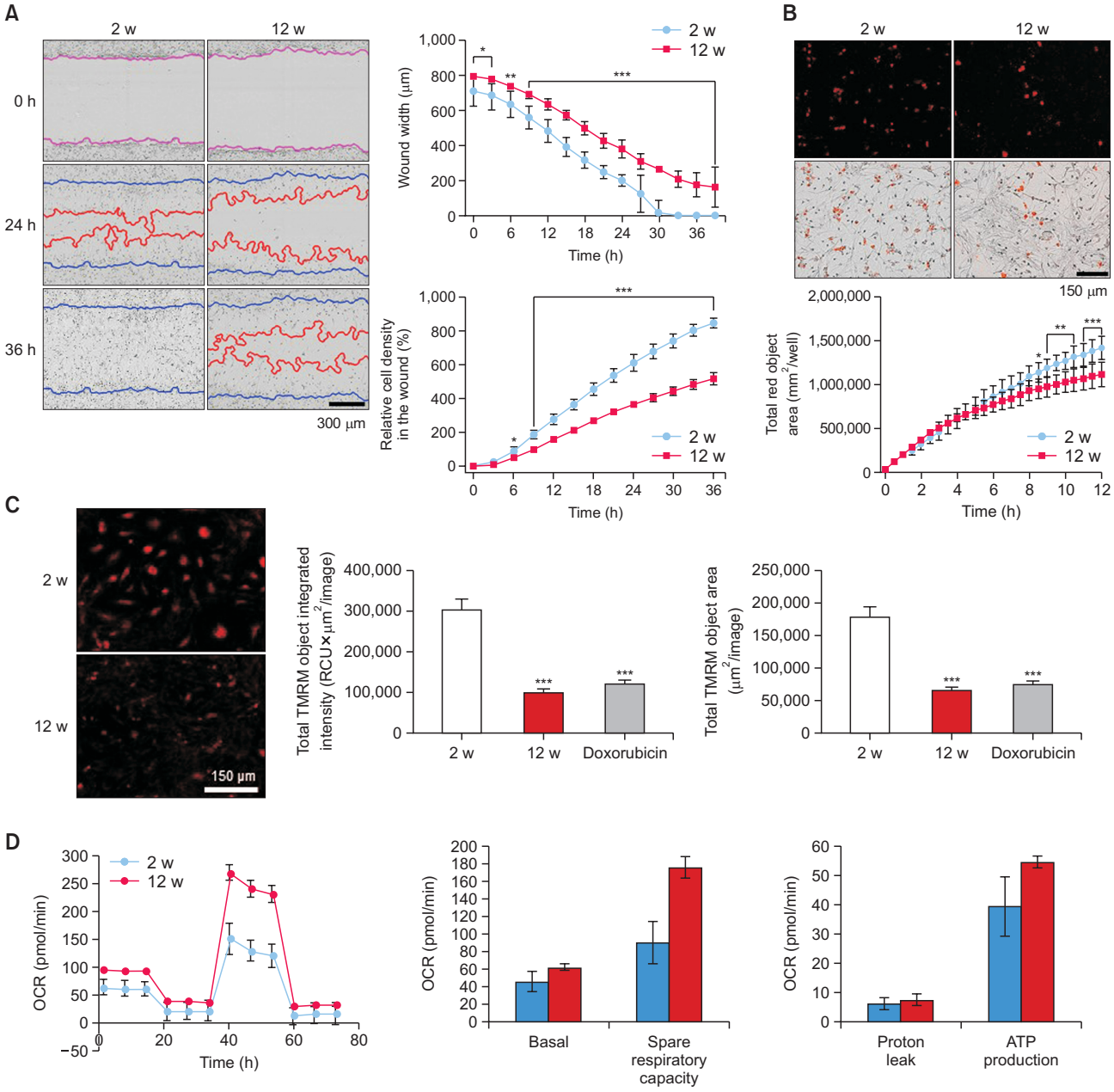

Fig. 3. Functional changes of long-term cultured astrocytes. (A) Cultured astrocytes were measured for migration ability through wound healing scratch assay. (B) Cells were confirmed phagocytosis using E. coli particles for 12 h. The cells were also checked for mitochondrial function by (C) mitochondrial membrane potential and (D) mitochondrial oxygen consumption rate (OCR). *p<0.05, **p<0.01, and ***p<0.001 vs. short-term cultured astrocytes. The data analysis was performed using two-way ANOVA and Error bars indicate SD.

sion in long-term cultured astrocytes. Among the perturbagens identified through CMap, candidates having the potential to regulate changes in long-term cultured astrocytes were selected and further investigated (Fig. 5B).

Minoxidil reverses phenotypic changes in long-term cultured astrocytes

We confirmed whether the functional dysregulation of long-term cultured astrocytes can be modulated by selected perturbagens identified with CMap analysis (Fig. 5B). We preliminarily screened several candidates and minoxidil showed most significant functional changes in long-term cultured astrocytes. During the long-term culture period, minoxidil was administered for the last 2 weeks, and it was examined whether the functional changes of astrocytes by long-term culture can be reversed. The number of SA-β-gal positive cells increased during long-term culture, which was significantly reduced by minoxidil treatment (Fig. 6A). In addition, the size of the nucleus was enlarged by long-term culture that was significantly reduced in the minoxidil-treated group (Fig. 6B). The size of nucleus in min-

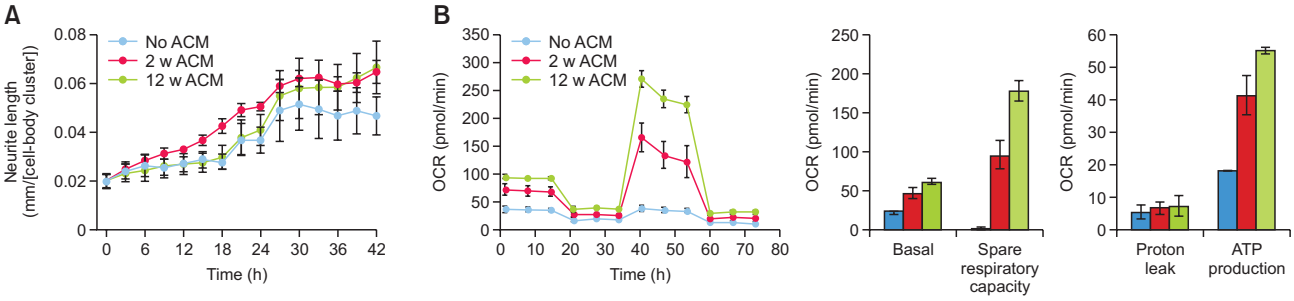

Fig. 4. Functional changes of cultured neurons by astrocytes conditioned media (ACM) treatment. Cultured cortical neurons were treated ACM. (A) The neurons were subjected to live cell imaging to check the neurite length for 42 h. (B) Mitochondrial OCR of neurons were measured using Cell Mito Test Kit (Agilent Technology) and Agilent Seahorse XFe96 Analyzer (Agilent Technology). The data analysis was performed using two-way ANOVA and Error bars indicate SD.

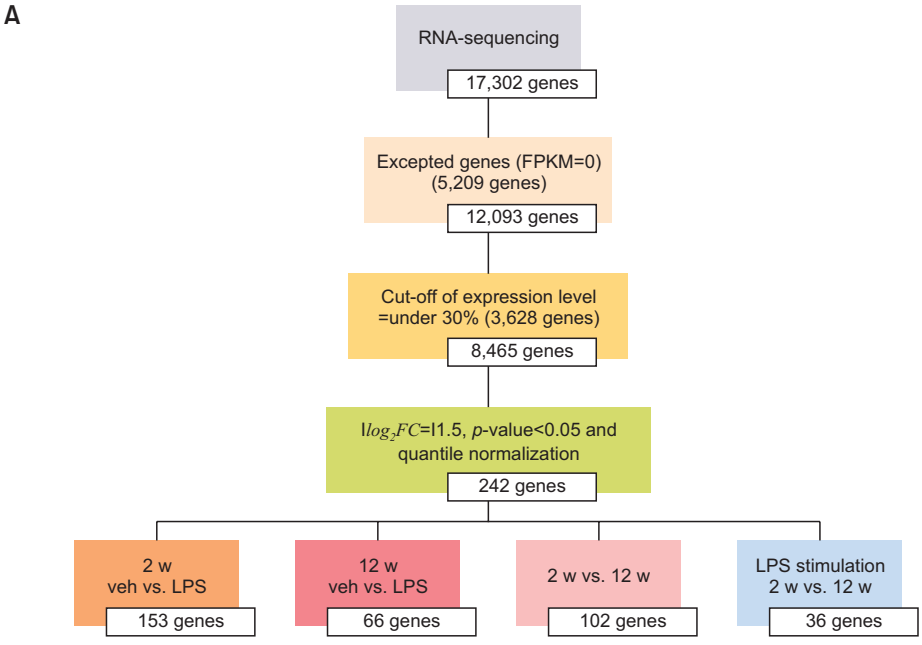

B

rank	cmap name	mean	n	enrichment	p	specificity	percent non-null
1	cefamandole	0.654	4	0.897	0.0001	0	100
2	econazole	0.595	4	0.829	0.00129	0.041	100
3	puromycin	-0.559	4	-0.829	0.00163	0.0373	100
4	vorinostat	-0.317	12	-0.515	0.00166	0.354	58
5	iproniazid	0.501	5	0.731	0.00318	0.0223	80
6	minoxidil	-0.383	5	-0.704	0.00503	0.0113	60
7	flupentixol	0.264	4	0.759	0.00631	0.0214	50
8	harmalol	0.621	3	0.85	0.00633	0	100
9	16,16-dimethylprostaglandin E2	-0.595	3	-0.853	0.00637	0.0138	100
10	diethylstilbestrol	0.497	6	0.636	0.00701	0.0842	83

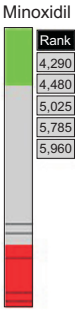

Fig. 5. Big data analysis of long-term cultured astrocytes. RNA-sequencing was performed on cultured astrocytes and analyzed. (A) RNA-sequencing results were analyzed following workflow. (B) Cmap used for finding novel therapeutics.

oxidil treated group was exhibited similar size with short-term cultured astrocytes (Fig. 6B). In the zymography experiments, the increased PAI-1 activity was normalized by minoxidil treatment (Fig. 7). The mitochondrial function was examined using MitoSOX™. The increased production of mitochondrial superoxide by long-term culture was mitigated in the minoxidil-treated

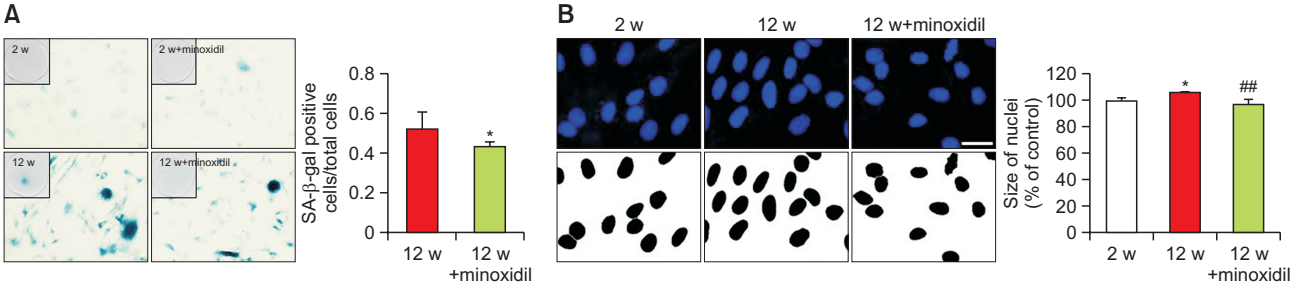

Fig. 6. Minoxidil reversed morphological changes on long-term cultured astrocytes. Long-term cultured astrocytes were pretreated with vehicle (DMSO) or 10 μM minoxidil before 2 weeks. (A) Cultured astrocytes were inspected for SA-β-gal positive cells. (B) Nuclei size were examined on cultured astrocytes. Scale bar=25 m. The graph shows nuclei size of cells. *p<0.05 vs. vehicle treated astrocytes. $^{\#\#}p$<0.001 vs. long-term cultured astrocytes. Error bars indicate SD.

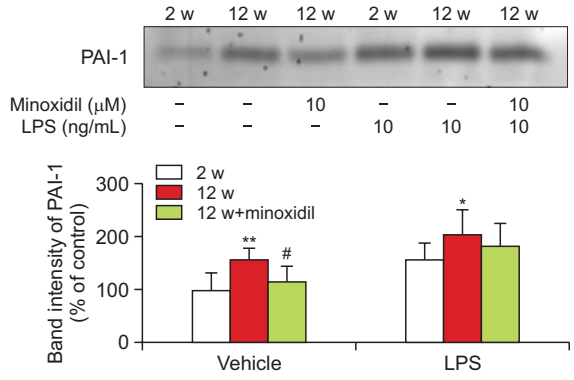

Fig. 7. Minoxidil reversed molecular changes on long-term cultured astrocytes. Long-term cultured astrocytes were pretreated with vehicle (DMSO) or 10 μM minoxidil for 2 weeks. Protein activity was examined through zymography and inverse-zymography. * indicates p<0.05, and ** indicates p<0.01 vs. short-term cultured astrocytes. $^{\#}p$<0.05 vs. long-term cultured astrocytes. Error bars indicate SD.

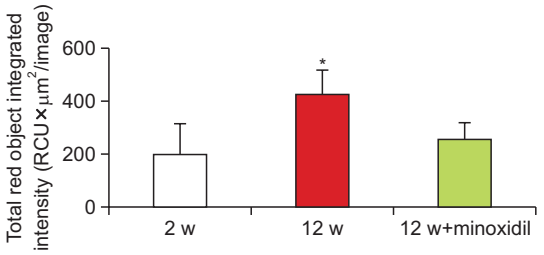

Fig. 8. Minoxidil reversed functional changes on long-term cultured astrocytes. Long-term cultured astrocytes were pretreated with vehicle (DMSO) or 10 μM minoxidil for 2 weeks. Mitochondrial superoxide was detected by MitoSOX dye. *p<0.05 vs. vehicle treated astrocytes. Error bars indicate SD.

group (Fig. 8). Taken together, the dysregulation of astrocyte functions by long-term culture was normalized by treatment with minoxidil.

DISCUSSION

In this study, cellular senescence of astrocytes was induced through long-term culture. We have previously reported the induction of cellular senescence of astrocytes using several different methods such as drug treatment or high-passage subculture *in vitro* (Bang *et al*., 2019a, 2019b, 2021). We examined morphological, molecular, and functional changes of astrocytes to confirm the face validity of the senescent model, which tells whether this model exhibits similar phenotypes with the aged cells. First, we determined the cellular senescence using SA-β-gal staining method. In addition to this morphological measure, we also determined the size of the nucleus using DAPI staining based on the studies suggesting the possibility of the increased cell or nucleus size in senescent cells as a result of the ageing-induced increased macromolecule contents (DNA, RNA, and proteins) (De Cecco *et al*., 2011). The SA-β-gal and nuclear staining data obtained from this study clearly indicates that long-term cultured cells exhibit the morphological features of senescent cells.

Senescent cells release senescence-associated secretory phenotype (SASP) such as cytokines, chemokines and growth factors (Elkhattouti *et al*., 2015; Palmer *et al*., 2015). Consistent with those reports, long-term cultured astrocytes displayed increased mRNA and/or protein expression of cytokines such as IL-6 and IL-1β as well as iNOS. In addition to these classical mediators of inflammation, extracellular matrix regulator and neuromodulator PAI-1 is increased in long-term cultured. PAI-1 is a member of the serine protease inhibitor (serpin) family and inhibits tissue plasminogen activator (tPA) and urokinase-type plasminogen activator (uPA), which might be related to its role in neurodegenerative diseases such as AD and ischemia (Nagai *et al*., 2005; Angelucci *et al*., 2019). It has been reported that PAI-1 is up-regulated in senescent cells as well as by immune stimulation (Elzi *et al*., 2012; Rana *et al*., 2020). The increased cytokine expression in our long-term cultured astrocytes may underlie the increased expression of PAI-1, which might contribute to the manifestation of neurodegenerative disorders. This interesting possibility should be investigated further in the future study.

p16 is a tumor suppressor that slows cell division by inhibiting CDK and is considered as a biomarker of cellular senescence (Hall *et al*., 2016). p16-expressing neuronal stem cells were identified in aged brains, and their expression is increased in aged mouse (Zou *et al*., 2012; Burd *et al*., 2013), which might be associated with decreased progenitor function (Molofsky *et al*., 2006). Interestingly, removal of p16-positive

cells delays the onset of aging or age-related diseases (Baker *et al*., 2008, 2011). Whether the increased expression of p16 in aged astrocytes as observed in this study contribute to the regulation of aging process per se and relative importance of stem cell senescence (or inhibition of proliferation) compared with astrocyte senescence on the development of neurodegenerative disorders awaits further investigation.

Functional examination of aged astrocytes in this study showed prominent defects in cell migration. In this regard, it is noteworthy that tPA and PAI-1 are well known targets and regulators of proliferation and migration pathways (Czekay *et al*., 2011) as well as aging and immune responses (Valentijn *et al*., 2018; Zhang *et al*., 2021). In addition, tPA and PAI-1 plays crucial roles in the regulation of neurite outgrowth (Xin *et al*., 2010; Lee *et al*., 2014; Yu *et al*., 2019). Considering the changes in the tPA and PAI-1 activity in this study, these proteins may underlie the dysregulation of migration of long-term cultured astrocytes, which hampers the regenerative potential of astrocytes after injury as well as the potential to poster neurite extension from damaged or newly generated neurons.

Mitochondrial dysfunction including mtDNA mutations, decreased mitochondrial potential. Actually, the imbalance in mitochondrial dynamics is regarded as one of the indicators of aging. (Sugrue and Tatton, 2001; Seo *et al*., 2010; Srivastava, 2017). The reduced mitochondrial membrane potential observed in this study, might be related to the increased non dividing cells at their G0 phase at which the mitochondrial membrane potential decreased (Sugrue and Tatton, 2001). In addition, senescent cells are resistant to metabolic challenge by increasing mitochondrial OCR to meet the energy demand (Kim *et al*., 2018b), which might adversely affect the cells by increased ROS accumulation and increased fusion of mitochondria (Son *et al*., 2017). Dysregulation of mitochondrial function may adversely affect astrocyte function, which in turn accelerate mitochondrial dysfunction that might perpetuate neural dysfunction in aged brain. In this study, spare respiratory capacity (SRC) is the component of mitochondrial OCR showing most prominent changes in aged astrocytes. It has been argued that SRC is the robust parameters to evaluate mitochondrial reserve and non-proliferative cells might have higher proliferative potential (Marchetti *et al*., 2020), consistent with the reduced proliferative potential of the aged astrocytes observed in this study. Interestingly it is also reported that higher SRC is related to the reduced nuclear reprogramming and hence the reduced iPSC induction capacity (Zhou *et al*., 2017). Whether the aged astrocytes may have defective roles in stem cell induction and proliferation needs to be explored in the future study.

Transcriptomic profiling using GENE MANIA and GOrilla, revealed major changes in cytokines/chemokines and related functions as well as regulations of extracellular regions. This is consistent with the previous research suggesting the upregulation of immune-related factors such as SASP with aging (Coppe *et al*., 2010; Davalos *et al*., 2010; Michaud *et al*., 2013; Cuollo *et al*., 2020). Interestingly, among the gene sets showing significantly reduced expression, those related with TNF production are identified. There are several reports that TNF is involved in wound-healing, neuronal survival and strengthening of synapses (Zhang *et al*., 2011; Ashcroft *et al*., 2012; Kim *et al*., 2018a; Heir and Stellwagen, 2020).

Through the CMap analysis and subsequent validation studies, minoxidil has been identified as a potential candidate to reverse or prevent astrocyte aging. Minoxidil is a pyrimidine derivative drug used to treat high blood pressure and hair loss. Interestingly, minoxidil has been implicated in neuroprotection, induction of cell growth factor, and stimulation of cell proliferation (Messenger and Rundegren, 2004; Chen *et al*., 2017). In addition, it has been reported that minoxidil modulates signaling pathways known to regulate cellular senescence such as insulin signaling pathways and mTOR, suggesting that these signaling pathways may contribute to reversing the phenotype of aged astrocytes including inflammation, mitochondrial dysfunction and abnormal proteostasis (Sanders *et al*., 1996; Campisi *et al*., 2019; Liu and Sabatini, 2020). Our results demonstrated that minoxidil normalized morphological phenotype and expression of immune-related factor as well as PAI-1 in long-term cultured astrocytes. Moreover, mitochondrial superoxide was reduced by minoxidil treatment in aged astrocytes raising the possibility that minoxidil can be used as a potential candidate to delay or inhibit the astrocyte aging. However, further studies are needed on the mechanism involved in reversing aged astrocytes.

In conclusion, we demonstrated that long-term culture can be used as an appropriate cell model for astrocyte aging research and for screening of anti-aging drugs. Genetic profiling analysis using aged astrocytes may provide us chances to excavate a potential therapeutic candidate against aging and various neurodegenerative diseases that is, in this case, minoxidil.

ACKNOWLEDGMENTS

This work was supported by the Brain Research Program (2019M3C7A1031455) and the Basic Science Research Program (2022R1A2C1005917) through the National Research Foundation (NRF) of Korea funded by the Ministry of Science, ICT & Future Planning, and the NRF grant funded by the Korea government (MSIT) (2016R1A5A2012284, 2017M3A9G2077568 and 2020M3E5D9080165).

REFERENCES

Abbott, N. J., Ronnback, L. and Hansson, E. (2006) Astrocyte-endothelial interactions at the blood-brain barrier. *Nat. Rev. Neurosci.* **7**, 41-53.

Angelucci, F., Cechova, K., Prusa, R. and Hort, J. (2019) Amyloid beta soluble forms and plasminogen activation system in Alzheimer's disease: consequences on extracellular maturation of brain-derived neurotrophic factor and therapeutic implications. *CNS Neurosci. Ther.* **25**, 303-313.

Ashcroft, G. S., Jeong, M. J., Ashworth, J. J., Hardman, M., Jin, W., Moutsopoulos, N., Wild, T., McCartney-Francis, N., Sim, D., McGrady, G., Song, X. Y. and Wahl, S. M. (2012) Tumor necrosis factor-alpha (TNF-alpha) is a therapeutic target for impaired cutaneous wound healing. *Wound Repair Regen.* **20**, 38-49.

Baker, D. J., Perez-Terzic, C., Jin, F., Pitel, K. S., Niederlander, N. J., Jeganathan, K., Yamada, S., Reyes, S., Rowe, L., Hiddinga, H. J., Eberhardt, N. L., Terzic, A. and van Deursen, J. M. (2008) Opposing roles for p16Ink4a and p19Arf in senescence and ageing caused by BubR1 insufficiency. *Nat. Cell Biol.* **10**, 825-836.

Baker, D. J., Wijshake, T., Tchkonia, T., LeBrasseur, N. K., Childs, B. G., van de Sluis, B., Kirkland, J. L. and van Deursen, J. M. (2011) Clearance of p16Ink4a-positive senescent cells delays ageing-associated disorders. *Nature* **479**, 232-236.

Bang, M., Gonzales, E. L., Shin, C. Y. and Kwon, K. J. (2021) Late pas-

sage cultivation induces aged astrocyte phenotypes in rat primary cultured cells. *Biomol. Ther. (Seoul)* **29**, 144-153.

Bang, M., Kim, D. G., Gonzales, E. L., Kwon, K. J. and Shin, C. Y. (2019a) Etoposide induces mitochondrial dysfunction and cellular senescence in primary cultured rat astrocytes. *Biomol. Ther. (Seoul)* **27**, 530-539.

Bang, M., Ryu, O., Kim, D. G., Mabunga, D. F., Cho, K. S., Kim, Y., Han, S. H., Kwon, K. J. and Shin, C. Y. (2019b) Tenovin-1 induces senescence and decreases wound-healing activity in cultured rat primary astrocytes. *Biomol. Ther. (Seoul)* **27**, 283-289.

Burd, C. E., Sorrentino, J. A., Clark, K. S., Darr, D. B., Krishnamurthy, J., Deal, A. M., Bardeesy, N., Castrillon, D. H., Beach, D. H. and Sharpless, N. E. (2013) Monitoring tumorigenesis and senescence *in vivo* with a p16(INK4a)-luciferase model. *Cell* **152**, 340-351.

Burda, J. E., Bernstein, A. M. and Sofroniew, M. V. (2016) Astrocyte roles in traumatic brain injury. *Exp. Neurol.* **275 Pt 3**, 305-315.

Campisi, J., Kapahi, P., Lithgow, G. J., Melov, S., Newman, J. C. and Verdin, E. (2019) From discoveries in ageing research to therapeutics for healthy ageing. *Nature* **571**, 183-192.

Chen, Y. F., Chen, L. H., Yeh, Y. M., Wu, P. Y., Chen, Y. F., Chang, L. Y., Chang, J. Y. and Shen, M. R. (2017) Minoxidil is a potential neuroprotective drug for paclitaxel-induced peripheral neuropathy. *Sci. Rep.* **7**, 45366.

Chung, W. S., Allen, N. J. and Eroglu, C. (2015) Astrocytes control synapse formation, function, and elimination. *Cold Spring Harb. Perspect. Biol.* **7**, a020370.

Coppe, J. P., Desprez, P. Y., Krtolica, A. and Campisi, J. (2010) The senescence-associated secretory phenotype: the dark side of tumor suppression. *Annu. Rev. Pathol.* **5**, 99-118.

Cuollo, L., Antonangeli, F., Santoni, A. and Soriani, A. (2020) The Senescence-Associated Secretory Phenotype (SASP) in the challenging future of cancer therapy and age-related diseases. *Biology (Basel)* **9**, 485.

Czekay, R. P., Wilkins-Port, C. E., Higgins, S. P., Freytag, J., Overstreet, J. M., Klein, R. M., Higgins, C. E., Samarakoon, R. and Higgins, P. J. (2011) PAI-1: an integrator of cell signaling and migration. *Int. J. Cell Biol.* **2011**, 562481.

Davalos, A. R., Coppe, J. P., Campisi, J. and Desprez, P. Y. (2010) Senescent cells as a source of inflammatory factors for tumor progression. *Cancer Metastasis Rev.* **29**, 273-283.

De Cecco, M., Jeyapalan, J., Zhao, X., Tamamori-Adachi, M. and Sedivy, J. M. (2011) Nuclear protein accumulation in cellular senescence and organismal aging revealed with a novel single-cell resolution fluorescence microscopy assay. *Aging* **3**, 955-967.

Dimri, G. P., Lee, X., Basile, G., Acosta, M., Scott, G., Roskelley, C., Medrano, E. E., Linskens, M., Rubelj, I., Pereira-Smith, O., Peacocke, M. and Campisi, J. (1995) A biomarker that identifies senescent human cells in culture and in aging skin *in vivo*. *Proc. Natl. Acad. Sci. U. S. A.* **92**, 9363-9367.

Dossi, E., Vasile, F. and Rouach, N. (2018) Human astrocytes in the diseased brain. *Brain Res. Bull* **136**, 139-156.

Elkhattouti, A., Hassan, M. and Gomez, C. R. (2015) Stromal fibroblast in age-related cancer: role in tumorigenesis and potential as novel therapeutic target. *Front. Oncol.* **5**, 158.

Elzi, D. J., Lai, Y., Song, M., Hakala, K., Weintraub, S. T. and Shiio, Y. (2012) Plasminogen activator inhibitor 1--insulin-like growth factor binding protein 3 cascade regulates stress-induced senescence. *Proc. Natl. Acad. Sci. U. S. A.* **109**, 12052-12057.

Fiacco, T. A., Agulhon, C. and McCarthy, K. D. (2009) Sorting out astrocyte physiology from pharmacology. *Annu. Rev. Pharmacol. Toxicol.* **49**, 151-174.

Freeman, S. H., Kandel, R., Cruz, L., Rozkalne, A., Newell, K., Frosch, M. P., Hedley-Whyte, E. T., Locascio, J. J., Lipsitz, L. A. and Hyman, B. T. (2008) Preservation of neuronal number despite age-related cortical brain atrophy in elderly subjects without Alzheimer disease. *J. Neuropathol. Exp. Neurol.* **67**, 1205-1212.

Hall, B. M., Balan, V., Gleiberman, A. S., Strom, E., Krasnov, P., Virtuoso, L. P., Rydkina, E., Vujcic, S., Balan, K., Gitlin, I., Leonova, K., Polinsky, A., Chernova, O. B. and Gudkov, A. V. (2016) Aging of mice is associated with p16(Ink4a)- and beta-galactosidase-positive macrophage accumulation that can be induced in young mice by senescent cells. *Aging* **8**, 1294-1315.

Heir, R. and Stellwagen, D. (2020) TNF-mediated homeostatic synaptic plasticity: from *in vitro* to *in vivo* models. *Front. Cell. Neurosci.* **14**, 565841.

Kim, M., Jung, K., Kim, I. S., Lee, I. S., Ko, Y., Shin, J. E. and Park, K. I. (2018a) TNF-alpha induces human neural progenitor cell survival after oxygen-glucose deprivation by activating the NF-kappaB pathway. *Exp. Mol. Med.* **50**, 1-14.

Kim, S. J., Mehta, H. H., Wan, J., Kuehnemann, C., Chen, J., Hu, J. F., Hoffman, A. R. and Cohen, P. (2018b) Mitochondrial peptides modulate mitochondrial function during cellular senescence. *Aging* **10**, 1239-1256.

Ko, H. M., Joo, S. H., Lee, S. H., Kim, H. J., Lee, S. H., Cheong, J. H., Ryu, J. H., Kim, J. M., Koo, B. N. and Shin, C. Y. (2015) Propofol treatment modulates neurite extension regulated by immunologically challenged rat primary astrocytes: a possible role of PAI-1. *Arch. Pharm. Res.* **38**, 556-565.

Lamb, J., Crawford, E. D., Peck, D., Modell, J. W., Blat, I. C., Wrobel, M. J., Lerner, J., Brunet, J. P., Subramanian, A., Ross, K. N., Reich, M., Hieronymus, H., Wei, G., Armstrong, S. A., Haggarty, S. J., Clemons, P. A., Wei, R., Carr, S. A., Lander, E. S. and Golub, T. R. (2006) The Connectivity Map: using gene-expression signatures to connect small molecules, genes, and disease. *Science* **313**, 1929-1935.

Lee, S., Kim, S., Kang, H. Y., Lim, H. R., Kwon, Y., Jo, M., Jeon, Y. M., Kim, S. R., Kim, K., Ha, C. M., Lee, S. and Kim, H. J. (2020) The overexpression of TDP-43 in astrocytes causes neurodegeneration via a PTP1B-mediated inflammatory response. *J. Neuroinflammation* **17**, 299.

Lee, S. H., Ko, H. M., Kwon, K. J., Lee, J., Han, S. H., Han, D. W., Cheong, J. H., Ryu, J. H. and Shin, C. Y. (2014) tPA regulates neurite outgrowth by phosphorylation of LRP5/6 in neural progenitor cells. *Mol. Neurobiol.* **49**, 199-215.

Liu, G. Y. and Sabatini, D. M. (2020) mTOR at the nexus of nutrition, growth, ageing and disease. *Nat. Rev. Mol. Cell Biol.* **21**, 183-203.

Marchetti, P., Fovez, Q., Germain, N., Khamari, R. and Kluza, J. (2020) Mitochondrial spare respiratory capacity: mechanisms, regulation, and significance in non-transformed and cancer cells. *FASEB J.* **34**, 13106-13124.

Messenger, A. G. and Rundegren, J. (2004) Minoxidil: mechanisms of action on hair growth. *Br. J. Dermatol.* **150**, 186-194.

Michaud, M., Balardy, L., Moulis, G., Gaudin, C., Peyrot, C., Vellas, B., Cesari, M. and Nourhashemi, F. (2013) Proinflammatory cytokines, aging, and age-related diseases. *J. Am. Med. Dir. Assoc.* **14**, 877-882.

Molofsky, A. V., Slutsky, S. G., Joseph, N. M., He, S., Pardal, R., Krishnamurthy, J., Sharpless, N. E. and Morrison, S. J. (2006) Increasing p16INK4a expression decreases forebrain progenitors and neurogenesis during ageing. *Nature* **443**, 448-452.

Nagai, N., Suzuki, Y., Van Hoef, B., Lijnen, H. R. and Collen, D. (2005) Effects of plasminogen activator inhibitor-1 on ischemic brain injury in permanent and thrombotic middle cerebral artery occlusion models in mice. *J. Thromb. Haemost.* **3**, 1379-1384.

Palmer, A. K., Tchkonia, T., LeBrasseur, N. K., Chini, E. N., Xu, M. and Kirkland, J. L. (2015) Cellular senescence in type 2 diabetes: a therapeutic opportunity. *Diabetes* **64**, 2289-2298.

Rana, T., Jiang, C., Liu, G., Miyata, T., Antony, V., Thannickal, V. J. and Liu, R. M. (2020) PAI-1 regulation of TGF-beta1-induced alveolar type II cell senescence, SASP secretion, and SASP-mediated activation of alveolar macrophages. *Am. J. Respir. Cell Mol. Biol.* **62**, 319-330.

Sanders, D. A., Fiddes, I., Thompson, D. M., Philpott, M. P., Westgate, G. E. and Kealey, T. (1996) In the absence of streptomycin, minoxidil potentiates the mitogenic effects of fetal calf serum, insulin-like growth factor 1, and platelet-derived growth factor on NIH 3T3 fibroblasts in a K+ channel-dependent fashion. *J. Invest. Dermatol.* **107**, 229-234.

Seo, A. Y., Joseph, A. M., Dutta, D., Hwang, J. C., Aris, J. P. and Leeuwenburgh, C. (2010) New insights into the role of mitochondria in aging: mitochondrial dynamics and more. *J. Cell Sci.* **123**, 2533-2542.

Siracusa, R., Fusco, R. and Cuzzocrea, S. (2019) Astrocytes: role and functions in brain pathologies. *Front. Pharmacol.* **10**, 1114.

Son, J. M., Sarsour, E. H., Kakkerla Balaraju, A., Fussell, J., Kalen, A. L., Wagner, B. A., Buettner, G. R. and Goswami, P. C. (2017) Mitofusin 1 and optic atrophy 1 shift metabolism to mitochondrial respiration during aging. *Aging Cell* **16**, 1136-1145.

Srivastava, S. (2017) The mitochondrial basis of aging and age-related disorders. *Genes* **8**, 398.

Sugrue, M. M. and Tatton, W. G. (2001) Mitochondrial membrane potential in aging cells. *Biol. Signals Recept.* **10**, 176-188.

Valentijn, F. A., Falke, L. L., Nguyen, T. Q. and Goldschmeding, R. (2018) Cellular senescence in the aging and diseased kidney. *J. Cell Commun. Signal.* **12**, 69-82.

Xin, H., Li, Y., Shen, L. H., Liu, X., Wang, X., Zhang, J., Pourabdollah-Nejad, D. S., Zhang, C., Zhang, L., Jiang, H., Zhang, Z. G. and Chopp, M. (2010) Increasing tPA activity in astrocytes induced by multipotent mesenchymal stromal cells facilitate neurite outgrowth after stroke in the mouse. *PLoS One* **5**, e9027.

Yoon, K. B., Park, K. R., Kim, S. Y. and Han, S. Y. (2016) Induction of nuclear enlargement and senescence by sirtuin inhibitors in glioblastoma cells. *Immune Netw.* **16**, 183-188.

Yu, P., Venkat, P., Chopp, M., Zacharek, A., Shen, Y., Liang, L., Landschoot-Ward, J., Liu, Z., Jiang, R. and Chen, J. (2019) Deficiency of tPA exacerbates white matter damage, neuroinflammation, glymphatic dysfunction and cognitive dysfunction in aging mice. *Aging Dis.* **10**, 770-783.

Zhang, H., Zheng, Q., Guo, T., Zhang, S., Zheng, S., Wang, R., Deng, Q., Yang, G., Zhang, S., Tang, L., Qi, Q., Zhu, L., Zhang, X. F., Luo, H., Zhang, X., Sun, H., Gao, Y., Zhang, H., Zhou, Y., Han, A., Zhang, C. S., Xu, H. and Wang, X. (2022) Metabolic reprogramming in astrocytes results in neuronal dysfunction in intellectual disability. *Mol. Psychiatry* doi: 10.1038/s41380-022-01521-x [Online ahead of print].

Zhang, L., Berta, T., Xu, Z. Z., Liu, T., Park, J. Y. and Ji, R. R. (2011) TNF-alpha contributes to spinal cord synaptic plasticity and inflammatory pain: distinct role of TNF receptor subtypes 1 and 2. *Pain* **152**, 419-427.

Zhang, M., Serna-Salas, S., Damba, T., Borghesan, M., Demaria, M. and Moshage, H. (2021) Hepatic stellate cell senescence in liver fibrosis: characteristics, mechanisms and perspectives. *Mech. Ageing Dev.* **199**, 111572.

Zhou, Y., Al-Saaidi, R. A., Fernandez-Guerra, P., Freude, K. K., Olsen, R. K., Jensen, U. B., Gregersen, N., Hyttel, P., Bolund, L., Aagaard, L., Bross, P. and Luo, Y. (2017) Mitochondrial spare respiratory capacity is negatively correlated with nuclear reprogramming efficiency. *Stem Cells Dev.* **26**, 166-176.

Zou, Y., Zhang, N., Ellerby, L. M., Davalos, A. R., Zeng, X., Campisi, J. and Desprez, P. Y. (2012) Responses of human embryonic stem cells and their differentiated progeny to ionizing radiation. *Biochem. Biophys. Res. Commun.* **426**, 100-105.